

Cross-Sectional Ballistic Electron Emission Microscopy for Schottky Barrier Height Profiling on Heterostructures

D. Rakoczy, G. Strasser, J. Smoliner

Institut für Festkörperelektronik & Mikrostrukturzentrum der TU-Wien
Floragasse 7, A-1040 Wien, Austria

In this work, Cross-Sectional Ballistic Electron Emission Microscopy (= "XBEEM") is introduced to determine a Schottky barrier height profile of a GaAs-AlGaAs multi heterostructure in cross-sectional geometry. Ballistic electron spectra measured across the heterostructure with nm resolution indicate that the measured Schottky barrier height profile is smeared out compared to the conduction band profile calculated from the sample growth parameters. We attribute this behavior to lateral band bending effects along the heterojunction. In addition, we have evidence that the barrier height profile is influenced by single impurities in the AlGaAs layers.

Introduction

Ballistic Electron Emission Microscopy (BEEM) [1], [2] is a three terminal extension of Scanning Tunneling Microscopy (STM) [3] – [5] where the STM tip is used to inject hot electrons into a semiconductor via a thin metallic base layer evaporated onto a semiconductor surface. If the electron energy is high enough to overcome the Schottky barrier height at the metal-semiconductor interface, the electrons can penetrate into the semiconductor. The corresponding current, measured vs. the tunneling bias using a backside collector contact, is called BEEM spectrum. By mapping the BEEM current for a constant tip bias while scanning the sample surface, images can be taken with a spatial resolution of about 1 nm. Presently, BEEM is a well established technique to determine Schottky barrier heights (SBH) and subsurface band offsets. An overview of this technique can be found in several review articles [6] – [8].

Cross-sectional STM techniques are widely used in surface physics. During the last years, it was found that cross-sectional STM techniques (XSTM) are especially helpful for the characterization of MBE (Molecular Beam Epitaxy) grown heterostructures. XSTM measurements, e.g. have resolved atomic features of segregated interfaces [9], [10]. More recently, special attention was given to XSTM on InAs-GaAs heterostructures, since they are the base material for self assembled quantum dots. On such samples, the local composition of the InAs dots and the wetting layer [11], [12] was studied by XSTM.

Surprisingly, and although it is a quite straightforward idea to combine cross-sectional STM techniques and BEEM, no cross-sectional BEEM (XBEEM) experiments have been reported in the literature until now. In our opinion, the reason for this is not a lack of application possibilities, but notable technical difficulties, e.g. the precise sample positioning and, especially for profile measurements, a state of the art compensation of piezo creep. Once these problems are overcome, XBEEM turns out to be a very useful technique to determine profiles of various band structure related features, e.g. the conduction band offsets of GaAs-AlGaAs multi heterostructures.

Experimental

In this paper, cross-sectional BEEM measurements are reported on the cleaved [011] surface of a GaAs-AlGaAs multi-heterostructure covered with gold. To test XBEEM as a new method for cross-sectional SBH profile measurements, we used an MBE grown GaAs-AlGaAs multiple barrier structure with relatively thick layers: On a semi insulating substrate (GaAs [100]), a 3 μm thick layer of n-type GaAs (silicon doped, $N_D = 8 \times 10^{16} \text{ cm}^{-3}$) was grown as a spacer. On top of this layer we grew 6 periods of an AlGaAs-GaAs heterostructure ($d_{\text{AlGaAs}} = 20 \text{ nm}$, $d_{\text{GaAs}} = 50 \text{ nm}$) followed by a 200 nm thick GaAs spacer. This layer sequence was repeated three times, however, with layer thicknesses of ($d_{\text{AlGaAs}} = 50 \text{ nm}$, $d_{\text{GaAs}} = 20 \text{ nm}$) and ($d_{\text{AlGaAs}} = 50 \text{ nm}$, $d_{\text{GaAs}} = 50 \text{ nm}$), respectively. The aluminum content was 30% for all AlGaAs layers. In order to use the sample in a BEEM configuration one has to provide means to collect the injected ballistic current. This was achieved by doping all GaAs layers with silicon ($N_D = 8 \times 10^{16} \text{ cm}^{-3}$) and the AlGaAs layers with $N_D = 5.6 \times 10^{16} \text{ cm}^{-3}$, which guarantees a sufficient collector conductance as well as a good Schottky contact.

To prepare the samples for BEEM, InSn pellets were alloyed into the sample to establish the collector contact. After that, the samples were cleaved in air and immediately transferred into a vacuum chamber. As base layer, a 7 nm thick gold film was evaporated onto the cleaved [011] surface at base pressures $< 1 \times 10^{-7}$ mbar using shadow evaporation techniques. After the evaporation process, the samples were glued on edge onto a sample transfer plate with conductive silver, which also provides the contact to the InSn pellets. An indium covered gold wire was attached to the gold covered [011] surface as a base contact. Finally, the sample was transferred as fast as possible into an Omicron Cryo SFM head. The scanning head is operated in helium atmosphere in a variable temperature inset of a cryostat. In this way, an undesired oxidation of the AlGaAs layers is suppressed. For all STM and BEEM measurements presented here, Au-coated ($d_{\text{Au}} \approx 10 \text{ nm}$) non-contact AFM-tips were used. All measurements were carried out at a temperature of $T = 200 \text{ K}$. This temperature is a very good compromise in meeting the requirements of minimizing piezo drift and sample degradation on the one hand and of a sufficiently large scan field and an optimal duty cycle of the bath cryostat on the other hand.

Results

The left hand side of Fig. 1 (a) shows a topographic image of the active region of our sample. The image was recorded at a tunneling current of $I_T = 2 \text{ nA}$ and a bias of $V_T = 1.6 \text{ V}$. Underneath the Au covered surface, the AlGaAs barriers are slightly visible as horizontal lines. The AlGaAs regions appear a little bit higher ($\approx 0.5 \text{ nm}$) than the GaAs regions, which is due to weak strain effects between the GaAs and the AlGaAs layers. The right hand side of Fig. 1 (a) shows the corresponding BEEM image. Here, the AlGaAs barriers are clearly visible as dark horizontal lines. Note that the samples are not stable and start to degrade after being stored in air for some days. A typical example for this can be seen in Fig. 1 (b): Here, the Au layer appears to be broken into fragments and in the corresponding BEEM image (Fig. 1 (b), right), the AlGaAs barriers are no longer clearly resolved and appear to have intermixed with the GaAs layers. In addition, the overall transmission is reduced approximately by a factor of 5 compared to a fresh sample. We attribute this behavior to an oxidation of the AlGaAs layers.

Figure 2 shows typical BEEM spectra acquired on a GaAs (curve (1)) and an AlGaAs region (curve (2)) on the cross-section of our sample. To show the onsets more clearly, we zoomed into the interesting data range. As common practice in BEEM, the current onsets were determined by a Bell Kaiser fit and are at $V_{b,\text{GaAs}} = 0.97 \text{ V}$ and $V_{b,\text{AlGaAs}} = 1.235 \text{ V}$, respectively. The difference $e\Delta V_b = 265 \text{ meV}$ is larger than the conduction band offset between GaAs and AlGaAs, which is $\Delta E_c = 230 \text{ meV}$ for $x = 30\%$ according

to the literature. Further note that these onset positions are about 50 meV higher compared to values commonly reported for conventional BEEM on [100] GaAs and AlGaAs samples. Possible explanations for this lie in the properties of the cleaved [011] surface and in the fact that the surface was not treated with HCl as it is usually done in conventional BEEM for oxide removal.

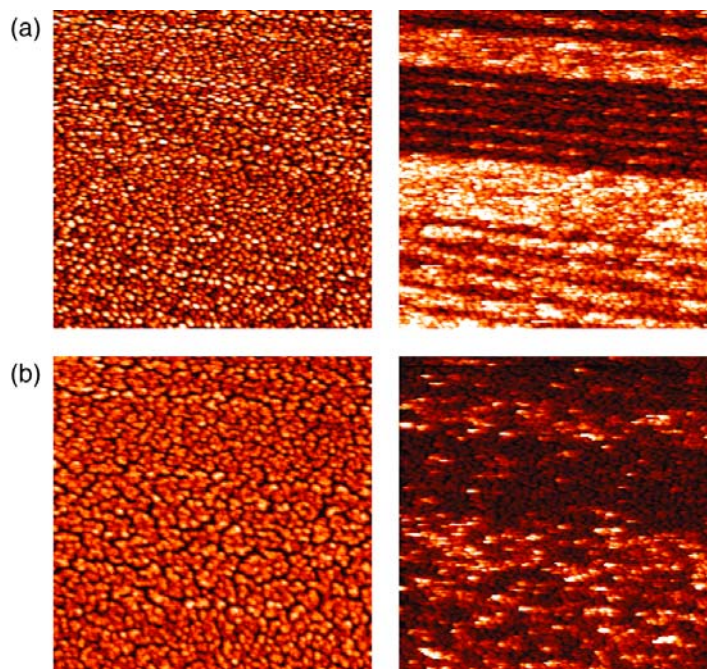


Fig. 1: (a), Left: Topographic STM image of the active region of our sample. Scan size is 1400 nm x 1400 nm. The z-scale is 4 nm. Tunneling current: $I_T = 2$ nA, bias $V_T = 1.6$ V. Right: Simultaneously recorded BEEM image. The color scale corresponds to BEEM currents of 0...2.5 pA. (b), Images of a degraded sample, same scan size as in (a). $I_T = 5$ nA, $V_T = 1.6$ V. Left: STM topography. The z-scale is 8 nm. Right: Simultaneously recorded BEEM image. The color scale corresponds to BEEM currents of 0...1.25 pA.

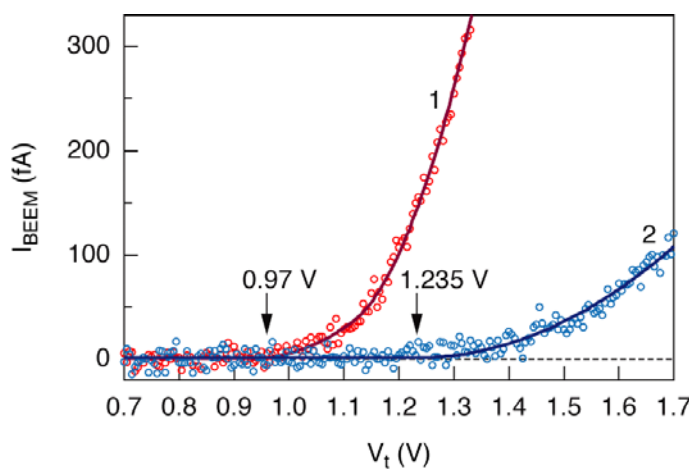


Fig. 2: Typical BEEM spectra acquired on a GaAs (curve (1)) and an AlGaAs region (curve (2)). The tunneling current was $I_T = 2$ nA and the temperature was $T = 200$ K. The onset bias is at 0.97 V and 1.235 V, respectively.

Figure 3 (top) shows a 143 nm x 45 nm large BEEM image taken in the area of an AlGaAs barrier. The barrier region is visible as dark area in this image, embedded by two brighter regions of GaAs. As typical for BEEM, the Au grains have a significant influence on the transmission. The total transmission is a convolution of the transmission of the granular Au layer and the barrier underneath, which makes it difficult to depict the sharp MBE grown GaAs-AlGaAs interface precisely. However, a different Au-coverage of the base layer does not influence the onset of the BEEM spectra, which is merely determined by the Schottky barrier height.

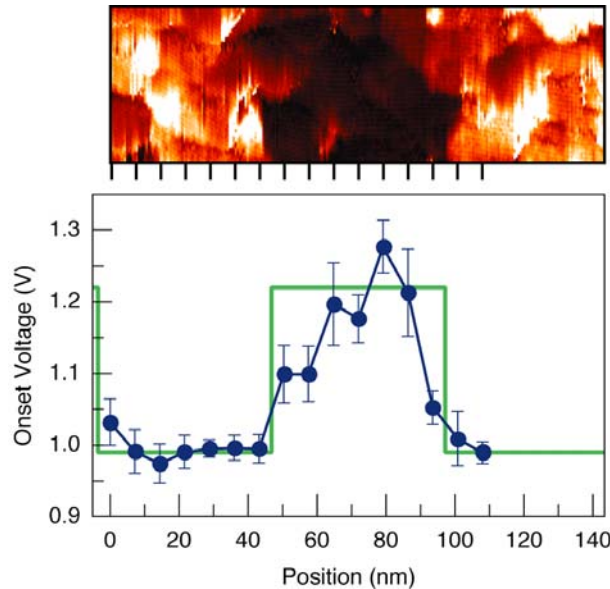


Fig. 3: Top: BEEM image of a AlGaAs barrier region, Scan size: 143 nm x 45 nm. $I_T = 2$ nA, $V_T = 1.7$ V. The color scale corresponds to current values from 0 pA ... 4 pA. Along the bottom line of this image, a series of BEEM spectra was recorded. The distance between the single points is 7.2 nm. Bottom: Measured Schottky barrier height profile determined from the BEEM spectra and the conduction band profile of the sample as calculated from the MBE growth parameters.

For a quantitative profile of the SBH across the heterostructure, a number of BEEM spectra ($I_T = 2$ nA) were recorded at the marked spots along the bottom line of the image in Fig. 3. From the onset of these spectra, the local barrier heights were determined using a Bell-Kaiser fit. The result of this procedure can be seen in the lower part of Fig. 3 together with a conduction band profile based on the heterostructure design parameters. For comparison with the GaAs-AlGaAs band offsets, this band profile was aligned with the measured SBH in the GaAs regions. Each data point of the measured curve represents an average over the onsets of several spectra taken at the same position. The error bars indicate the standard deviation in the measured onset at each position. The lateral distance between the single data points is 7.2 nm.

As one can see, the barrier is depicted clearly in the profile. The barrier width is consistent with the BEEM image as well as with the growth parameters. However, the barrier height profile is not rectangular, as it would be expected from a conduction band profile obtained from the MBE growth parameters, and also exhibits a certain asymmetry. In addition, the maximum barrier height difference between GaAs and AlGaAs differs notably from the expected conduction band offset between GaAs and AlGaAs. Furthermore, the noise in the barrier height profile is significantly larger in the AlGaAs regions than in the GaAs areas on our sample.

Before the origins of the above features are discussed, we would like to point out that we can definitely exclude two possible experimental artifacts: First of all, the smeared out barrier height profile is not due to the limited lateral resolution of BEEM. As already confirmed in previous measurements, the typical resolution of BEEM is about 1nm. This is also verified by Fig. 3 (a), where BEEM contrast is achieved on such length scales. In contrast to that, the smeared out region in the barrier height profile is significantly larger.

Second, the higher noise in the barrier height profile in the AlGaAs regions is definitely not due to improper tunneling conditions. As one can see in Fig. 1 (a), the sample is very flat and the image quality is good everywhere. Also the noise in the BEEM spectra is equal for all regions (see Fig. 2) and the noise in the barrier height profile in the GaAs regions is comparable to what we are used from earlier measurements on reference samples. Thus, we conclude, that this effect is a genuine feature of the local properties of the AlGaAs layer.

In our opinion, the smeared out barrier height profile is most likely due to lateral band bending effects across the heterojunctions based on the following arguments: In general it can not be expected that the GaAs-AlGaAs conduction band offset is exactly mirrored by the difference in the SBH of the two materials. This is confirmed by our data, where the SBH on some points of the AlGaAs layers is notably larger than the SBH on GaAs plus the band offset between GaAs and AlGaAs. On the other hand, the Fermi level must be constant all over the sample surface and thus lateral band bending effects are unavoidable. A quantitative analysis of this behavior, however, requires extensive simulation as well as additional systematic measurements and is beyond the scope of this paper.

While lateral band bending can explain the amount of broadening on the right edge of the barrier profile seen in Fig. 3, it does not explain the rather gradual increase on the left edge of the profile. Also the increased noise in the AlGaAs regions is still an open issue. However, a look on earlier measurements, where we investigated the local influence of single impurities in AlAs barriers in BEEM [13], can shed light on this behavior. In that work we found that in the vicinity of an impurity the onset of the BEEM current was reduced from the Schottky barrier height of AlGaAs to the energetic level of the impurity.

Considering the design of our present sample, the AlGaAs barriers are doped with $N_D = 5.6 \times 10^{16} \text{ cm}^{-3}$, which means that the average distance between two impurities is $\approx 33 \text{ nm}$. Thus, on average, one to four impurities are present in the vicinity of any cross-section through a 50 nm thick AlGaAs barrier.

While in GaAs silicon impurity levels are close to the conduction band edge, they act as deep donors in AlGaAs. As shown in our previous work, the local influence of these impurities on the current onset position is quite dominant, which probably is the reason why the corresponding AlGaAs barrier height depends so strongly on the position on our sample. In contrast to that, the donor levels on GaAs are just 5 meV below the conduction band edge and therefore have almost no influence on the local barrier height. This is consistent with our experimental observation that the barrier height shows just little variations throughout the GaAs regions of our sample.

Summary

In summary, cross-sectional BEEM measurements were introduced to determine a Schottky barrier height profile on the cleaved [011] surface of a GaAs-AlGaAs multi-heterostructure. The measured data exhibit indications of lateral band bending effects at the GaAs-AlGaAs interfaces. Furthermore, an influence of deep impurity levels in the AlGaAs barriers on the measurements was observed.

Acknowledgements

This work was sponsored by “Fonds zur Förderung der wissenschaftlichen Forschung (FWF)” project No P16337-N08 and “Gesellschaft für Mikro- und Nanoelektronik (GMe)”

References

- [1] W.J. Kaiser and L.D. Bell, *Phys. Rev. Lett.* 60, 1406 (1988)
- [2] L.D. Bell and W.J. Kaiser, *Phys. Rev. Lett.* 61, 2368 (1988)
- [3] G.Binnig, G.Rohrer, Ch.Gerber, E.Weibel, *Phys. Rev. Lett.* 49, 57 (1982)
- [4] R.Wiesendanger, *Scanning Probe Microscopy and Spectroscopy*, Cambridge University Press (1994)
- [5] C. Julian Chen, *Introduction into Scanning Tunneling Microscopy*, Oxford Series in Optical and Imaging Sciences, Oxford University Press (1993)
- [6] M.Prietsch, *Physics Reports* 253, 163 (1995)
- [7] V.Narayanamurti and M.Kozhevnikov, *Physics Reports* 349, 447 (2001)
- [8] J.Smoliner, D.Rakoczy, M.Kast, *Rep. Prog. Phys.* 67, 1863 (2004)
- [9] J.Harper, M.Weimer, D.Zhang, C.H.Lin, S.S.Pei, *J.Vac. Sci. Technol. B*16, 1389 (1998).
- [10] R.Magri, A.Zunger, *Phys. Rev.* B64, 081305/1-4 (2001)
- [11] D.M.Bruls, P.M.Koenraad, M.Hopkinson, J.H.Wolter, H.W.M.Salemink, *Appl. Surf. Sci.* 190, 258 (2002)
- [12] S.L.Zuo, E.T.Yu, A.A.Allerman, R.M.Biefeld, *J.Vac. Sci. Technol. B*17, 1781 (1999)
- [13] D.Rakoczy, G.Strasser, J.Smoliner, *Phys. Rev.* B68, 073304 (2003)